# DESIGN OF HIGH EFFICIENCY HLE SOLAR CELLS FOR SPACE AND TERRESTRIAL APPLICATIONS*

A. Neugroschel and F. A. Lindholm
Department of Electrical Engineering
University of Florida

## SUMMARY

A first-order analysis of HLE cells is presented for both beginning-of-life (BOL) and end-of-life (EOL) conditions. Based on this analysis and on experimentally observed values for material parameters, we present design approaches for both space and terrestrial cells. The approaches result in specification of doping levels, junction depths and surface conditions. The proposed structures are projected to have both high $V_{OC}$ and high $J_{SC}$, and consequently high $\eta$.

## 1. INTRODUCTION

The purpose of this paper is to discuss design approaches for silicon HLE solar cells. Design of cells for radiation and terrestrial environments are considered. Two main types of HLE cells receive attention: (a) the oxide-charge-induced (OCI) HLE cell, and (b) a new HLE cell having a wide p-epitaxial emitter for which the appropriate choices of emitter width and doping levels in the emitter and base are made to yield both high $V_{OC}$ and high $J_{SC}$.

## SYMBOLS

| | |
|---|---|
| $D_a$ | ambipolar diffusivity ($cm^2$/sec) |
| $D_n$, $D_p$ | electron and hole diffusivities ($cm^2$/sec) |
| $Q_0$ | oxide charge density ($C/cm^2$) |
| $J_{SC}$ | short circuit current density ($A/cm^2$) |
| $J_{n0}$, $J_{p0}$ | dark electron and hole saturation current density ($A/cm^2$) |
| $L_n$, $L_p$ | electron and hole diffusion length (cm) |
| $\Delta n$,$\Delta p$ | excess electron and hole concentration ($cm^{-3}$) |

*This work was supported by NASA Grant NSG-3018.

| | |
|---|---|
| $n_i$ | intrinsic carrier concentration ($cm^{-3}$) |
| $n_s, P_s$ | electron and hole surface concentration ($cm^{-3}$) |
| $n_s(Q_0)$ | oxide charge dependent electron surface concentration ($cm^{-3}$) |
| $N_{DD}$, $N_{DD}^+$ | donor concentration in n and $n^+$ material ($cm^{-3}$) |
| $N_{AA}$, $N_{AA}^+$ | acceptor concentration in p and $p^+$ material ($cm^{-3}$) |
| q | electronic charge (Coulombs) |
| $S_p$ | hole surface recombination velocity (cm/sec) |
| $S_{eff}$ | effective surface recombination velocity (cm/sec) |
| T | temperature ($^oC$,$^oK$) |
| $V_A$ | applied voltage (Volts) |
| $V_{OC}$ | open circuit voltage (Volts) |
| $(V_{OC})_B$, $(V_{OC})_E$ | open circuit voltage established by base and emitter (Volts) |
| $W_E$ | emitter thickness (cm) |
| $X_j$ | junction depth (cm) |
| $\rho$ | resistivity ($\Omega$ cm) |
| $\tau_n, \tau_p$ | lifetime of minority electrons and holes (sec) |
| p, $p^+$ | associated with p and $p^+$ region |
| n, $n^+$ | associated with n and $n^+$ region |
| BOL | beginning-of-life |
| EOL | end-of-life |
| E, B | associated with emitter and base |

## II. OCI-HLE CELL

Fig. 1(a) shows the cross-section of an OCI silicon HLE solar cell. The principles of operation of this cell, which have previously been discussed [1] are illustrated in Figs. 1(a) and 1(b). A positive charge $Q_0$, achieved by suitable heat treatment [2,3], induces an electron accumulation and an electric field near the silicon surface which reduces the effective surface recombination velocity for holes $S_{eff}$ to [4]

$$S_{eff} \simeq \frac{N_{DD}}{n_s} S_p \qquad (1)$$

By solving the hole continuity equation for the desired case, $W_E < L_p$, and low injection, one determines the hole saturation current $J_{PO}$ to be [4]

$$J_{PO} \simeq \frac{qn_i^2}{N_{DD}} \left[ \frac{S_{eff} + \frac{W_E}{\tau_p}}{1 + \frac{S_{eff}}{D_p/W_E}} \right] \qquad (2)$$

in which the first term in the numerator accounts for hole recombination at the surface and the second term accounts for hole recombination in the bulk. The current $J_{PO}$ must be small if high $V_{OC}$ is to result.

### 2.1 Beginning of life - (BOL) Design

For BOL, our experiments [1] show that $S_p < 10^4$ cm/sec can result from the presence of the $SiO_2$ layer on the illuminated surface. For a wide range of doping levels $N_{DD}$, the term $W_E/\tau_p$ in (2) can be made negligible, and the diffusion velocity $D_p/W_E$ will typically be of the order of $10^4$ cm/sec. Thus, if $S_{eff}$ can be made much less than $10^4$ cm/sec, then (2) reduces to

$$J_{PO} \simeq \frac{qn_i^2}{N_{DD}} S_{eff} \simeq qn_i^2 \frac{S_p}{n_s} \qquad (3)$$

which also holds for high injection provided $D_a/W_E$ and $W_E/(\tau_n+\tau_p)$ are both small compared with $(S_{eff})_{high\ injection} = (n_i/n_s) \exp qV_A/2kT$, as can be shown by solving the ambipolar transport equation for high injection [5]. To show that $S_{eff} < 10^4$ cm/sec is possible, we indicate in Fig. 2, for different values of $N_{DD}$ and $Q_0$, the resulting values of $n_s$ and $S_{eff}$. The functional dependence $n_s(Q_0)$ is found from standard MOS theory [6].

Because $S_{eff}$ can be small, we consider now the value of $J_{PO}$ for the limiting case $S_{eff} = 0$. Fig. 1(b) shows the minority hole density in the dark cell, resulting from an applied voltage, for the desired condition, $L_p > W_E$:

$$J_{PO} \simeq qn_i^2 \, W_E(N_{DD}\tau_p)^{-1} \qquad (4)$$

To estimate $J_{PO}$, we use the empirical data of Kendall [7], which gives, for $N_{DD} \geqq 5 \times 10^{16} cm^{-3}$,

$$\tau_p N_{DD} \simeq 3 \times 10^{12} \text{ sec cm}^{-3} \qquad (5)$$

Thus, at $T = 25^oC$,

$$J_{p0} \simeq 7 \times 10^{-12}\ W_E \qquad (6)$$

Thus, if $J_{SC} \simeq 35\ mA/cm^2$ (AMO), which was seen in OCI-HLE cells, the open-circuit voltage limit, $(V_{OC})_E = kT/q\ \ell n(J_{SC}/J_{p0})$, established by the emitter current $J_{p0}$ is, for example, 800 mV, 780 mV, and 718 mV for $W_E$ = 2 μm, 5 μm, and 50 μm, respectively, independent of $N_{DD}$ (provided low-injection levels are maintained). From a design viewpoint, this demonstrates that $(V_{OC})_E > 700$ mV can be achieved for a wide variety of choices of $N_{DD}$ and $W_E$ provided only that $L_p > W_E$.

## 2.2 End-of-Life (EOL) Design

Radiation damage increase $S_p$ and $Q_0$[8]; it will also reduce $\tau_p$[9,10]. As a design approach, we choose $W_E$ small compared with anticipated degraded diffusion length to minimize bulk recombination; that is, we require $W_E < L_p$ (after irradiation). Then (2) still applies, and $J_{p0}$ is determined by the velocities $S_{eff}$, $W_E/\tau_p$, and $D_p/W_E$. As a worst-case limit, we consider the case $S_{eff} = \infty$. Then the transit time $t_t$ for holes to cross the emitter is

$$t_t = W_E^2/2D_p \qquad (7)$$

which, for example, is of the order of $10^{-9}$ sec for $W_E \simeq 2$ μm. Thus, if $\tau_p$ after irradiation is larger than $10^{-9}$ sec, the emitter will be transparent to holes and (2) reduces to

$$J_{p0} = \frac{qn_i^2}{N_{DD}} \frac{D_p}{W_E} \qquad (8)$$

This worst-case dependence suggests that $N_{DD}$ should be large enough, both to assure small lateral series resistance and to decrease $J_{p0}$, but small enough to avoid heavy-doping degradation. For example, consider a design with $W_E$ = 2 μm, and $N_{DD} = 10^{18}\ cm^{-3}$. For $T = 25^oC$ and $J_{SC} \simeq 25\ mA/cm^2$, $(V_{OC})_E > 640$ mV. For electron fluences up to $10^{15}\ cm^{-2}$, $J_{SC} \simeq 25\ mA/cm^2$ is expected if prior to radiation $J_{SC} \simeq 35\ mA/cm^2$ [10].

## 2.3 Examples of $V_{OC}$ established by the emitter for BOL and EOL

We have previously discussed $(V_{OC})_E$ for two limiting cases: $S_{eff} = 0$,

which corresponds to the BOL condition, and $S_{eff} = \infty$, which corresponds to the EOL condition. We now remove these limiting-case assumptions by considering intermediate values of $S_{eff}$, as determined by (1) and the condition that $10^3$ cm/sec $< S_p < 10^7$ cm/sec. The lower bound on $S_p$ is easily achieved, as is indicated by our experiments for a surface passivated by $SiO_2$ [1]. The upper bound is a theoretical limit for a silicon surface [11].

In Fig. 3 we plot $(V_{OC})_E$ as a function of $S_p$ for two values of emitter widths $W_E$ = 2.5 μm and 15 μm and for emitter doping densities of $N_{DD} = 10^{17}$ $cm^{-3}$ and $10^{18}$ $cm^{-3}$. Three values of oxide charge densities are considered: (a) $Q_0/q = 4 \times 10^{11}$ $cm^{-2}$, which is the order of magnitude obtained in thermally grown dry oxides followed by oxygen heat treatment at about 700 C [2,3] before the irradiation; and $Q_0/q = 1 \times 10^{12}$ $cm^{-2}$ and $5 \times 10^{-12}$ $cm^{-3}$, which is the range of values expected after irradiation [8]. As shown in Fig. 3 for BOL with $S_p \simeq 10^3$ cm/sec, the emitter recombination is no barrier for achieving $(V_{OC})_E \geqq 700$ mV for variety of emitter doping levels and thicknesses. After irradiation, for EOL, $S_p$ is expected to increase significantly [8], but will not be larger than the order of $10^6$ cm/sec [11]. But $Q_0/q$ will also increase, as mentioned above, which will increase $n_s$ [6], and $S_{eff} \simeq N_{DD}\, S_p/n_s\,(Q_0)$ will depend on the ratio $S_p/n_s\,(Q_0)$ after the irradiation. It follows from Fig. 3, consistent with our previous worst-case calculation, that $(V_{OC})_E > 650$ mV is still possible at EOL, if $W_E < (L_p)_{EOL}$.

### 2.4 $V_{OC}$ established by the base for BOL and EOL

As shown in Fig. 1(b) for the dark case with applied voltage $V_A$, the quasi-neutral saturation current $J_0$ in low injection, neglecting heavy-doping effects [12], is $J_0 = J_{p0} + J_{n0}$, and the base saturation current is

$$J_{n0} = \frac{qn_i^2 D_n}{N_{AA} L_n} \qquad (9)$$

To minimize $J_{n0}$, note that, for $N_{AA} \gtrsim 10^{17}$ $cm^{-3}$, $D_n/N_{AA}L_n$ is a decreasing function of $N_{DD}$[13], provided heavy doping effects are negligible. As a result, the open-circuit voltage limited by the base $(V_{OC})_B$ is an increasing function of $N_{DD}$ until $N_{AA} \simeq 10^{19}$ $cm^{-3}$ ($\rho_{base} \simeq 0.01$ Ωcm) which is a doping level at which the heavy doping effects in p-type material become important [12], as shown in

Fig. 4. The broken line in Fig. 4 shows an experimental dependence of $V_{OC}$ on $N_{AA}$ [14] which peaks at $N_{AA} \simeq 5 \times 10^{17}$ $cm^{-3}$. This is a result of the increasing importance of the emitter current $J_{p0}$, for base dopings larger than about $5 \times 10^{17}$ $cm^{-3}$, in conventional cell where the emitter current is not suppressed by an HLE structure such as that present in the proposed device.

## 3. Design concepts for space and terrestrial applications

Based on the foregoing analysis we present design concepts for two different types of space cells and for a terrestrial cell.

1) $n^+$-n-p OCI-HLE (diffused HLE) space cell

Fig. 5 shows a cell designed for space applications. The p-type base doping is $N_{AA} \simeq 5 \times 10^{17}$ ($\rho \simeq 0.1$ Ωcm) which appears to be an optimum value which gives $L_n$ in a range of 85-150 μm in a finished cell [15]. This long diffusion length, which will assure collection of most of the generated minority electrons, provides a high value of the short circuit current $J_{SC}$. The epitaxial emitter is narrow, about 2 μm, and highly doped, $N_{DD} \simeq 10^{17}$ to $10^{18}$ $cm^{-3}$, to assure low series resistance. The thinness of the emitter offsets, to a large degree, the effects of significant degradation of lifetime in the n-type material after the irradiation [9]. The H-L emitter junction can be achieved using either OCI induced or diffused $n^+$ layer [16].

The following conclusions about this structure can be made based on the discussion in the previous sections:

a) $(V_{OC})_E > 650$ mV at EOL, if $t_t < (\tau_p)_{EOL}$.

b) $(V_{OC})_B$ at EOL will depend on the radiation damage [10]. Since the base is the same as in the conventional n on p cell, results obtained for the conventional cell radiation damage [10] also apply here.

c) $(J_{SC})_{EOL} = (J_{SC})_{\substack{conventional \\ base}} + (J_{SC})_E$ .

d) For an OCI structure, $S_{eff} \simeq N_{DD} S_p/n_s$, where both $S_p$ and $n_s$ increase with radiation, thus tending to keep $S_{eff}$ low. $S_{eff}$ controls $(J_{SC})_E$ and $J_{p0}$.

e) For BOL, with $S_p \simeq 10^3$ cm/sec, $(V_{OC})_E > 700$ mV, and $(V_{OC})_B$ depends on minimizing $D_n/L_n\ N_{AA}$. $(V_{OC})_B$ of the order of 700 mV can be expected for $\rho_{base} \simeq 0.1$ Ωcm with $L_n > 75$ μm.

f) For $Q_0/q > 10^{12}$ cm$^{-2}$, heavy doping effects in the accumulation layer may become important [Fig. 2]. However, since the accumulation layer is very narrow, these effects are expected to be very small [17].

g) A structure with a diffused $n^+$-region offers larger flexibility in choosing $N_{DD}$ because of the low shunting resistance of the $n^+$-diffused layer.

2) A wide-emitter $p^+$-p-$n^+$ space cell

We propose a new silicon solar cell structure [18] which is projected to have both high $J_{SC}$(45 mA/cm$^2$) and high $V_{OC}$(700 mV) and consequently high $\eta$ (20%, AM0). The new structure is projected to have good performance in radiation as well as non-radiation environments.

The structure is shown in Fig. 6. The qualitative sketches showing the minority carrier distributions in Fig. 1 are valid for this case, too, with hole and electron profiles reversed.

We emphasize some special features of this structure:

a) The surface is passivated with $SiO_2$ on top of which a suitable antireflection (AR) coating is deposited. The H-L emitter junction is achieved by a thin ($\sim$0.1 μm) $p^+$-diffused layer resulting in [4]

$$S_{eff} \simeq S_n \frac{N_{AA}}{(N_{AA}^+)_{eff}} \qquad (10)$$

where $(N_{AA}^+)_{eff} \simeq 10^{19}$ cm$^{-3}$ is the effective doping in the $p^+$-diffused layer for $N_{AA}^+ \simeq 10^{20}$ cm$^{-3}$ at the surface. An electron recombination velocity at the Si-$SiO_2$ interface on the order of $10^3$ or less can be easily achieved [1]. Therefore, for $N_{AA} = 5 \times 10^{17}$ cm$^{-3}$, $S_{eff}$ is of the order of 10 cm/sec or less; thus $S_{eff} \simeq 0$ is a reasonable approximation.

b) As a result of $S_{eff} \simeq 0$, and the choice of a 50 μm wide emitter region, about 90% [19] of all available optically generated minority electrons will be collected. Using a 5% loss AR coating and 4% metal coverage the projected AM0 $J_{SC} \simeq 45$ mA/cm$^2$. P-type material is chosen as a region from which the $J_{SC}$ is collected due to smaller sensitivity to the radiation than seen in n-type material [9].

c) The doping level in the $n^+$-base is optimized to be about $10^{18}$ cm$^{-3}$, which is the onset level for heavy-doping effects [17]. The doping

level in the emitter ($\sim$5 x $10^{17}$ cm$^{-3}$) is chosen to minimize $N_{AA}\tau_n$ [13].

d) Using published data for lifetimes for holes and electrons [7,13], we can calculate by use of Eqs. (2) and (9), for structure shown in Fig. 6, that the saturation current $J_0 \lesssim 7 \times 10^{-14}$ A/cm$^2$, implying $V_{OC} \simeq 700$ mV for $J_{SC} = 45$ mA/cm$^2$ at 25°C, and implying $\eta \simeq 20\%$ AMO.

e) Significant differences exist between this new cell and a previously proposed epitaxial $p^+$-p-n cell [20]; these are discussed in detail in Ref. 18.

f) An alternative related structure ($p^+$-p-n-$n^+$) can be made, which employs an n-$n^+$ low-high junction back-surface-field base [4]. This structure will have higher $J_{SC}$ at BOL due to improved collection of minority holes from the n-region of the base.

3) <u>$n^+$-n-p OCI-HLE terrestrial cell (Fig. 1)</u>

There are two approaches to minimize the base current in this cell, Fig. 7:

a) Choose $\rho_{base} \simeq 0.1$ Ωcm ($N_{AA} \simeq 5 \times 10^{17}$ cm$^{-3}$). In this case $L_n \gtrsim 70$ μm is required for $(V_{OC})_B \simeq 700$ mV (25°C and $J_{SC} = 35$ mA/cm$^2$). Such values for $L_n$ can be achieved in finished cells using a low temperature fabrication process [13,15]. Epitaxial growth of the emitter and a high-temperature oxidation required for low $S_p$ [1] may decrease $L_n$ below the 70 μm; this would result in $(V_{OC})_B < 700$ mV. The largest $V_{OC}$ seen experimentally for a cell with $\rho_{base} \simeq 0.1$ Ωcm is 643 mV AMO, at 25°C.

b) A second approach is to use a highly doped p-type (5 x $10^{18}$ - $10^{19}$cm$^{-3}$) base. Note that for $N_{AA} = 5 \times 10^{18}$ cm$^{-3}$, for example, $L_n \simeq 2$ μm is sufficient to achieve $(V_{OC})_B$ of 700 mV. Such values are expected even after the high-temperature fabrication steps. In this second approach, $W_E \simeq 50$ μm, since the base will contribute negligibly to $J_{SC}$. Such a wide emitter is required to collect about 90% of generated minority holes. In approach (a), $W_E$ can range from about 10 to 50 μm. The largest $V_{OC}$ seen experimentally for a cell with $\rho_{base} \simeq 0.024$ Ωcm ($N_{AA} \simeq 2.5 \times 10^{18}$ cm$^{-3}$) is 647 mV AMO, at 25°C.

c) Emitter doping can be chosen from range of about 5 x $10^{16}$ cm$^{-3}$ to about 5 x $10^{17}$ cm$^{-3}$.

## CONCLUDING REMARKS

First order analysis of HLE solar cells for BOL and EOL conditions is presented. Based on this analysis and on experimentally measured material parameters, design concepts for both space and terrestrial cells are discussed. The proposed structures include: $n^+$-n-p OCI-HLE space cell, wide emitter $p^+$-p-$n^+$ space cell, and $n^+$-n-p OCI-HLE terrestrial cell. All structures are projected to yield both high $V_{OC}$ and $J_{SC}$.

REFERENCES


1. Neugroschel, A., Lindholm, F. A., Pao, S. C, and Fossum, J. G., "Emitter Current Suppression in a High-Low-Junction Emitter Solar Cell Using An Oxide-Charge-Induced Electron Accumulation Layer," Appl. Phys. Letters, vol. 33, July 15, 1978, pp. 168-170.

2. Deal, B. E., Sclar, M., Grove, A. S., and Snow, E. H., "Characteristics of the surface-state charge ($Q_{SS}$) of thermally oxidized silicon, J. Electrochem. Soc., vol. 114, March 1967, pp. 266-274.

3. Fu, H. S. and Sah, C. T., "Theory and experiments on surface 1/f noise", IEEE Trans. Electron Devices, vol. ED-19, Feb. 1972, 273-285.

4. Godlewski, M. P., Baraona, C. R., and Brandhorst, H. W., "Low-high junction theory applied to solar cells", in Record of Tenth IEEE Photovoltaic Specialist Conf., 1973.

5. Lindholm, F. A., Fossum, J. G., and Burgess, E. L., "Application of the superposition principle to solar-cell analysis", IEEE Trans. Electron Devices, vol. ED-26, March 1979, pp. 165-171.

6. Kingston, R. H. and Neustandter, S. F., "Calculation of the space charge, electric field and free carrier concentration at the surface of semiconductors, J. Appl. Phys., vol. 26, June 1955, pp. 718-720.

7. Kendall, D., Conf. Physics and Application of Lithium Diffused Silicon, NASA-Goddard Space Flight Center, Dec. 1969.

8. Zaininger, K. H. and Holmes-Siedle "A survey of radiation effects in metal-insulator-semiconductor devices", RCA Rev., vol. 28, 1967, pp. 208-241.

9. Cooley, W. C. and Janda, R. J., "Handbook of space-radiation effects on solar-cell power systems", NASA Report SP-3003, 1963.

10. Tada, H. Y. and Carter, J. R., "Solar cell radiation handbook", JPL Publication 77-56, 1977.

11. Heasell, E. L., "Recombination beneath ohmic contacts and adjacent oxide covered regions", Solid-State Electron., vol. 22, Jan. 1979, pp. 89-93.

12. Dunbar, P. M. and Hauser, J. R., "Theoretical effects of surface diffused region lifetime models on silicon solar cells", Solid-State Electron., vol. 20, August 1977, pp. 697-701.

13. Iles, P. A. and Soclof, S. I., "Effect of impurity doping concentration on solar cell output, in Record of Eleventh Photovoltaic Specialist Conf., 1975, pp. 19-24.

14. Godlewski, M. P., Brandhorst, H. W., and Baraona, C. R., "Effects of high doping levels on silicon solar cell performance", in Record of Eleventh Photovoltaic Specialists Conf., 1975, pp. 32-35.

15. Brandhorst, H. W. and Godlewski, M. P., private communication.

16. Lindholm, F. A., Neugroschel, A., Pao, S. C., Fossum, J. G., Sah, C. T., "Design Considerations for Silicon HLE Solar Cells", in Record of Thirteenth IEEE Photovoltaic Specialists Conf., 1978, pp. 1300-1305.

17. Lanyon, H. P. D. and Tuft, R. A, "Bandgap narrowing in heavily doped silicon", IEDM Technical Digest, Dec. 1978, pp. 316-319.

18. Neugroschel, A. and Lindholm, F. A., submitted for publication to IEEE Trans. Electron Devices.

19. Fossum, J. G., "Computer-aided numerical analysis of silicon solar cells", Solid-State Electron., vol. 19, April 1976, pp. 269-277.

20. D'Aiello, R. V., Robinson, P. H., and Kressel, H., "Epitaxial silicon solar cells", Appl. Phys. Letters, vol. 28, 15 Feb., 1976, pp. 231-234.

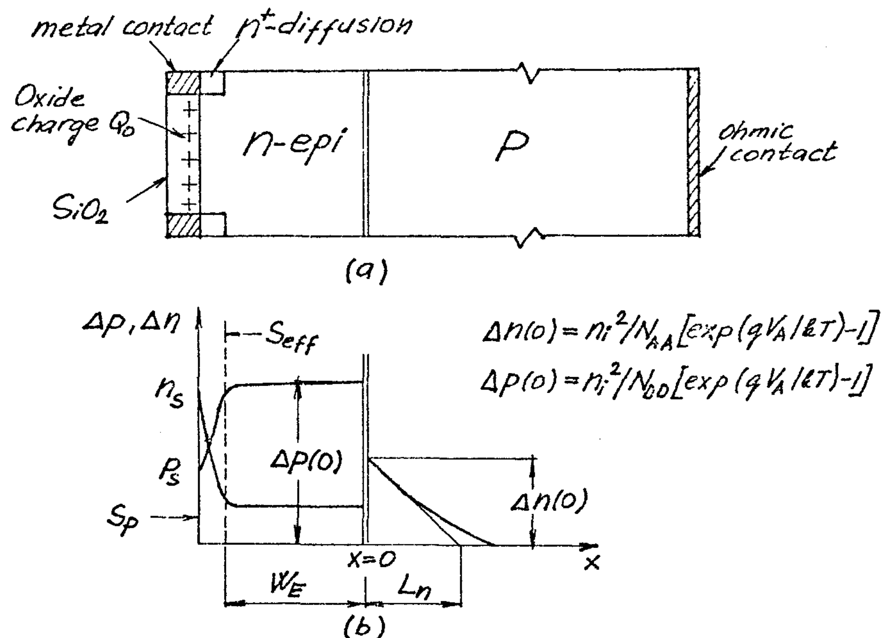


Fig. 1. (a) Schematic diagram of a $n^+$-n-p OCI-HLE cell.
(b) Qualitative sketches of excess minority carrier distribution in dark with applied voltage $V_A$.

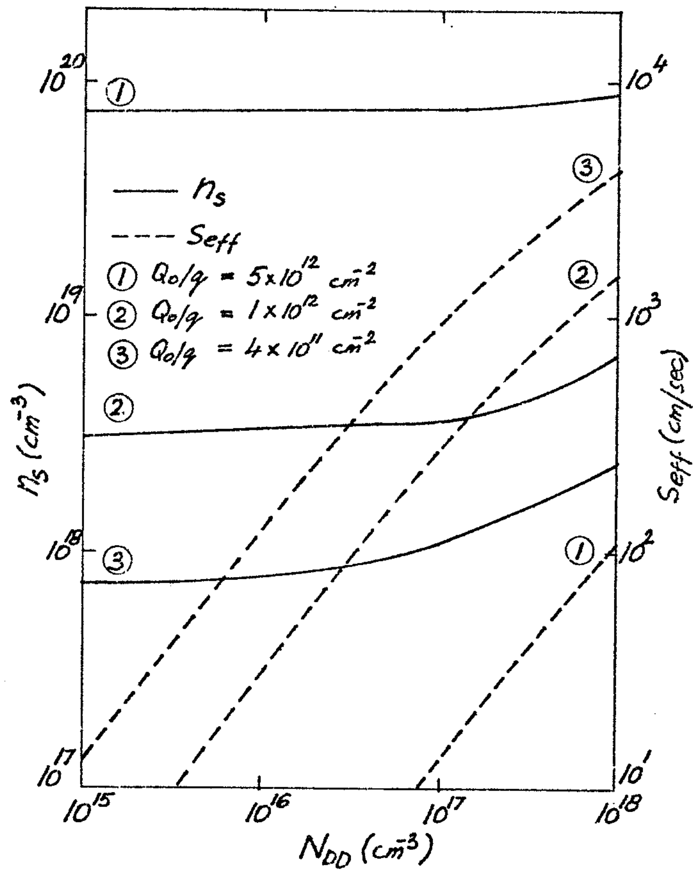


Fig. 2. Dependence of electron surface concentration $n_s$ and effective surface recombination velocity $S_{eff}$ (for $S_p = 10^4$ cm/sec) on emitter doping.

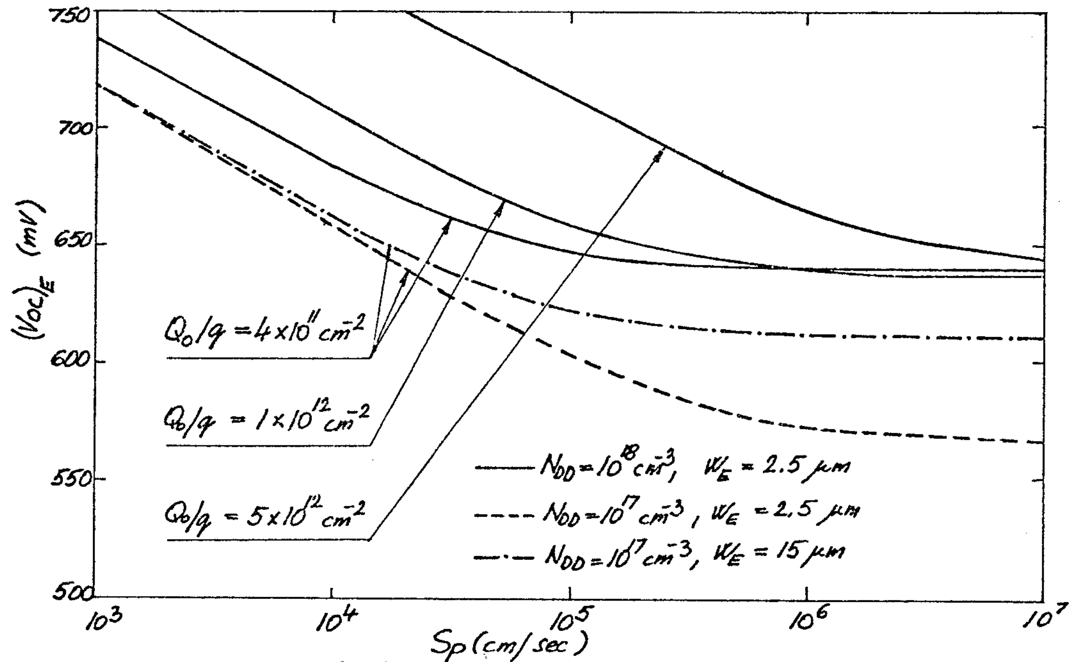


Fig. 3. Dependence of $(V_{oc})_E$ on $S_p$.

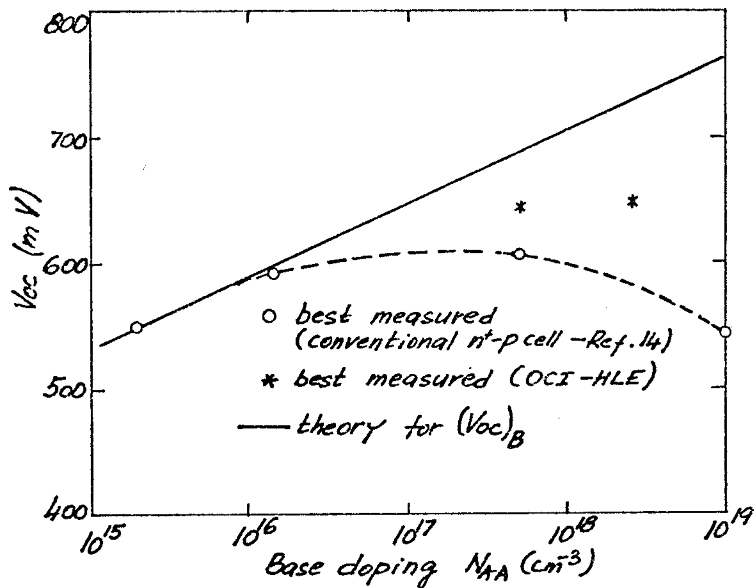


Fig. 4. Experimental and theoretical dependence of $V_{oc}$ on base doping. Best results obtained on OCI-HLE cells are 643 mV for 0.1 Ωcm base resistivity and 647 mV for 0.024 Ωcm base resistivity (measured at NASA Lewis, at 25°C, AM0).

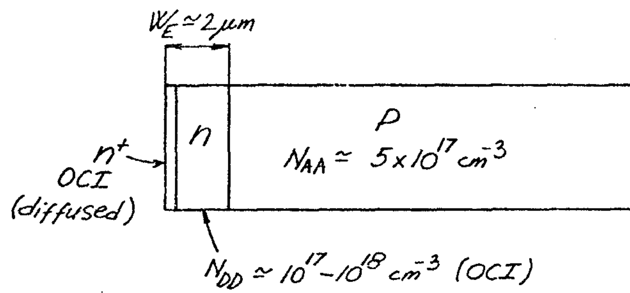


Fig. 5. Schematic diagram of a $n^+$-n-p OCI-HLE (diffused HLE) space cell.

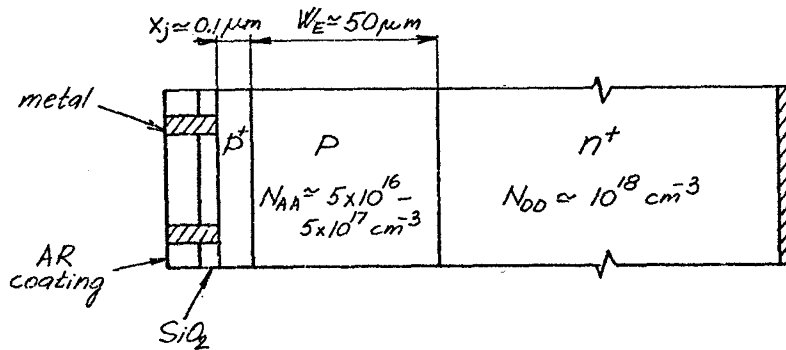


Fig. 6. Schematic diagram of a $p^+$-p-$n^+$ space cell.

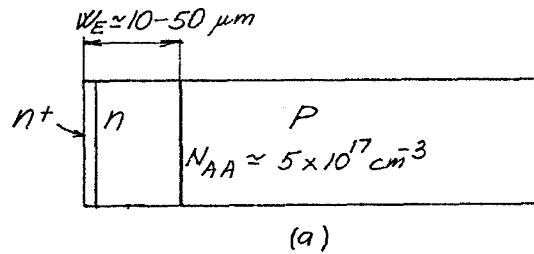


(a)

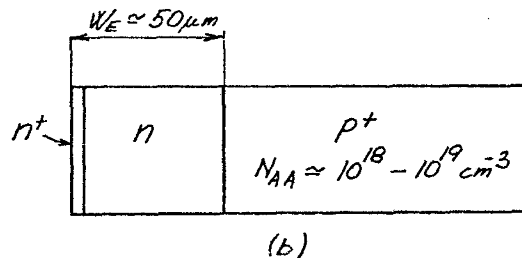


(b)

Fig. 7. Schematic diagrams of an OCI-HLE terrestrial cells.
(a) $n^+$-n-p cell
(b) $n^+$-n-$p^+$ cell